Operational mode-shape normalisation with a structural modification for small and light structures

Domen Rovšček[a], Janko Slavič[a], Miha Boltežar[a]

[a]*Laboratory for Dynamics of Machines and Structures, Faculty of Mechanical Engineering, University of Ljubljana, Aškerčeva 6, 1000 Ljubljana, Slovenia-EU.*
Corresponding author:
Miha Boltežar, miha.boltezar@fs.uni-lj.si,
Phone: +386 1 4771 608, Fax:+386 1 2518 567.

Abstract

When dealing with small and light structures, difficulties occur when measuring the modal parameters. The resonant frequencies are usually relatively high and therefore a wide frequency range is needed for the measurement. Furthermore, the mass that is added to the structure by the sensors causes structural modifications. To overcome these difficulties, an improved method using an operational modal analysis instead of an experimental modal analysis is proposed in this study. It is derived from the sensitivity-based operational mode-shape normalisation with a consideration of the mode-shape variation. The measurement of the excitation force is not needed, because the operational modal analysis is used and only two simultaneous response measurements at an unknown excitation are required. The proposed method includes the cancellation of the added mass, resulting in mode shapes and

resonant frequencies of the unmodified structure. The numerical and experimental results on small and light structures are compared with the results of the experimental modal analysis. The comparison shows that the proposed approach allows measurements over a wide frequency range and increases the accuracy of the results compared to the sensitivity-based operational mode-shape normalisation and also compared to the particular experimental modal analysis method that was used in this study. The advantages of the proposed method can be seen whenever the mass that is added to the structure by the accelerometer is not negligible and therefore a variation of the mode shapes occurs.

1. Introduction

Modal analyses are used to identify modal parameters (resonant frequencies, mode shapes and damping) [1, 2, 3]. The experimental modal analysis (EMA) [2], with a simultaneous measurement of the excitation force and the response of the structure, is the prevailing technique. If the excitation force and the response of the structure are known, the frequency-response functions (FRFs) can be calculated and the identification of the mass-normalised mode shapes (independent of the excitation) is possible. The operational modal analysis (OMA), on the other hand, is a technique for performing a modal analysis when the structure is excited by unknown operational loads. It was initially used as an addition to FRF measurements to define the modal parameters of the structure during the operation [4]. OMA was also employed

2

in rare cases, when people were dealing with large structures and a controlled excitation was hard to achieve [5], which means that only a modal identification with unknown operating loads was possible. The main drawback of OMA in comparison with EMA is that it cannot identify the mass-normalised mode shapes [6] and the main advantage is that an excitation-force measurement is not needed for the OMA, which simplifies the experimental procedure.

The EMA is, in some cases, extremely hard to perform due to accessibility difficulties or the characteristics (dimensions, mass) of the measured structure [7]. One example of this is when relatively small and light structures (mass < 50 gram) are measured. The main reason is the mass added to the structure by the transducers (force sensor, accelerometer), which changes the structure's modal characteristics. This effect was researched by Huber *et al.* [8], Ozdoganlar *et al.* [9], Silva *et al.* [10], Rovšček *et al.* [11], and others. In [11] a light, custom-made, force sensor, which adds only 0.4 grams to the structure was used. The sensor can operate at high frequencies (up to 20 kHz), which is suitable for small structures, because they usually have higher resonant frequencies [9]. OMA was rarely used on small and light structures in the past, especially because the mode shapes could not be mass normalised and therefore the modal description of the structure was not complete [2]. But in 2002 a new method was introduced by Parloo *et al.* [12], which makes the mass normalisation of the operational mode shapes possible. The operational mode shapes are normalised by multiplying them by scaling factors, which are derived from the modal sensitivity of the structure on a change of the mass matrix. Therefore, the term mass-change strategy is frequently used to denote Parloo's method. This mass-change strategy does

not require the measurement of the excitation force and it was first used on larger structures, for instance on a bridge [13], on a sprayer boom [14, 15], etc. The possibility and difficulties of using the mass-change strategy on small and light structures have not yet been analysed in detail.

The mass-change strategy works with the presumption that the resonant frequencies shift, but the mode shapes remain almost the same when the mass is added to the structure, as shown by Parloo *et al.* [12]. The results are relatively good, when the quantity of the added mass is just right (about 5 % of the whole mass of the structure), as Lopez-Aenlle *et al.* [16] concluded. Furthermore, the added mass needs to be well distributed over the structure. But when measuring small and light structures, the added mass can be too high and not well distributed. For this reason, not only do the resonant frequencies shift, but the mode shapes also change.

In this study an improved method that takes into account the mode-shape variation due to accelerometer added mass is presented. The normalisation of the operational mode shapes is based on a sensitivity analysis and a structural modification of the modal parameters. Two simultaneous measurements of the response are needed (for the OMA) and the excitation force is unknown. The reference response is measured by a lightweight accelerometer and the second response measurement is performed by a Laser Doppler Vibrometer (LDV). The results of the proposed operational mode-shape normalisation method are compared to the results of the EMA procedure presented by Rovšček *et al.* in [11] and to the numerical model. The method proposed in this study gives significantly better results than the EMA, especially at low frequencies (under 500 Hz), and is simpler to use, since the measurement of

the excitation force is not needed. It can be used on any similar small and light structure.

Parloo *et al.* [13, 14] tested larger structures and the masses of the accelerometers were very small compared to the measured structures. Therefore, the mass-loading effect of the accelerometers was negligible. However, when measuring small and light structures this effect is significant and it should be compensated in the modal analysis. The main advantage of the method presented in this study compared to the sensitivity-based operational mode-shape normalisation proposed by Parloo *et al.* [12] is that it also takes into account the mode-shape variation, which occurs due to the added mass of the accelerometer. There is also a possibility of using only non-contact measuring devices (like LDVs) for the measurement to avoid the mass-loading of the structure; however, in some cases the LDVs cannot be used. For instance, by a laser beam unreachable crevices due to application environment and/or fixation setup. In addition, the measurements at high frequencies with relatively small vibration amplitudes can easily reach the limit of the LDV's dynamic range. Therefore, the approach proposed in this study is applicable.

This study is organised as follows. Section 2 presents the theoretical background of this paper. The sample that was used for the numerical model and the measurements is presented in Section 3. The numerical model and its results are described in Section 4. Section 5 presents the experiments (EMA and OMA) and the comparison of the experimental and numerical results. A summary of the work is given in Section 6.

2. Theoretical background

2.1. Sensitivity-based operational mode-shape normalisation

The operational mode shapes are not mass normalised, since the excitation force is not measured when performing the OMA. Therefore, a new approach was proposed by Parloo *et al.* [12] to mass normalise the operational mode shapes on the basis of the modal sensitivity of the structure. The main idea of the method proposed by Parloo *et al.* is to normalise the measured mode shapes by multiplying them by scaling factors. By adding a known mass to the selected points of the structure the resonant frequencies shift. From these shifts the scaling factors for each mode shape can be calculated using the sensitivity analysis. The term mass-change strategy is frequently used to denote this method.

The use of the modal sensitivity to properly scale the operational mode shapes was later more thoroughly analysed by other researchers. Lopez-Aenlle *et al.* [17, 18, 16, 19], Fernandez *et al.* [20, 21] and others [22] gave suggestions about how to accurately normalise the mode shapes using different types of mass-change strategies. In [17] the equations for the calculation of the scaling factors were analysed and an iterative procedure for better accuracy was developed by Lopez-Aenlle *et al.* In [19] the influence of the location, number and size of the added masses on the accuracy of the results was analysed by Lopez-Aenlle *et al.* and experimentally verified in [20] by Fernandez *et al.*, who gave additional instructions on how to perform accurate calculations of the scaling factors in [16]. In [21] a new mass-change approach, which is based on using several sets of individual mass changes to estimate the scaling factors, was presented by Fernandez *et al.* Recently,

6

Khatibi *et al.* [23] and Lopez-Aenlle *et al.* [24] analysed the possibility of using a mass-and-stiffness change strategy with the sensitivity analysis for the mass normalisation of the operational mode shapes. All the listed methods for the operational mode-shape normalisation are based on the modal sensitivity of the structure.

Modal sensitivity describes the influence of the structural modification on the modal parameters of the structure. The modal sensitivity of the i-th resonant frequency ω_i and the mode shape $\{\phi_i\}$ are defined in [2], as shown in Equations (1) and (2), where p_j represents one of the N_p structural modifications.

$$\Delta\omega_i^2 \;\;=\;\; \sum_{j=1}^{N_p} \frac{\partial\omega_i^2}{\partial p_j} p_j \tag{1}$$

$$\Delta\{\phi_i\} \;\;=\;\; \sum_{j=1}^{N_p} \frac{\partial\{\phi_i\}}{\partial p_j} p_j \tag{2}$$

The mass-change strategy is based on Equation (1), as shown by Parloo *et al.* [12]. If the structural modifications p_j are the changes of mass at different points of the structure, then they can be described by a change of the mass matrix $[\Delta M]$. A known mass $[\Delta M]$ needs to be added to the structure to perform the mass-change strategy. The change of the mass matrix causes a variation of the modal parameters. If the modal parameters of the unmodified and modified structure are measured, then the scaling factors α_i can be calculated as shown in Equation (3):

$$\alpha_i = \sqrt{\frac{(\omega_i^2 - \omega_{i,M}^2)}{\omega_{i,M}^2 \{\psi\}^T [\Delta M]\{\psi\}}} \tag{3}$$

where ω_i denotes the i-th resonant frequency of the unmodified structure and $\omega_{i,M}$ is the i-th resonant frequency of the modified structure (when the mass

[ΔM] is added). $\{\psi\}$ is the unnormalised mode shape of the structure. A detailed derivation of (3) can be found in [17], where a presumption is made that the mode shapes do not change significantly when adding the mass to the structure ($\{\psi\} \approx \{\psi_i\} \approx \{\psi_{i,M}\}$). The mass-normalised mode shapes $\{\phi_i\}$ can then be obtained by multiplying the unnormalised mode shapes $\{\psi_i\}$ by the scaling factors α_i:

$$\{\phi_i\} = \alpha_i\{\psi_i\} \tag{4}$$

Equation (3) can be adjusted to include the modified $\{\psi_{i,M}\}$ or the unmodified $\{\psi_i\}$ mode shapes, as shown in Equations (5), (6) and (7), derived by Lopez-Aenlle et $al.$ [17]:

$$\alpha_{i,00} = \sqrt{\frac{(\omega_i^2 - \omega_{i,M}^2)}{\omega_{i,M}^2\{\psi_i\}^T[\Delta M]\{\psi_i\}}} \tag{5}$$

$$\alpha_{i,01} = \sqrt{\frac{(\omega_i^2 - \omega_{i,M}^2)}{\omega_{i,M}^2\{\psi_i\}^T[\Delta M]\{\psi_{i,M}\}}} \tag{6}$$

$$\alpha_{i,11} = \sqrt{\frac{(\omega_i^2 - \omega_{i,M}^2)}{\omega_{i,M}^2\{\psi_{i,M}\}^T[\Delta M]\{\psi_{i,M}\}}} \tag{7}$$

where $\alpha_{i,00}$ is calculated using only the unmodified mode shapes, $\alpha_{i,01}$ is the modified and unmodified mode shapes and $\alpha_{i,11}$ is just the modified mode shapes. All three scaling factors $\alpha_{i,00}$, $\alpha_{i,01}$ and $\alpha_{i,11}$ give accurate results. In some cases (like in this study) only the mode shapes $\{\phi_i\}$ of the unmodified structure or only the mode shapes $\{\phi_{i,M}\}$ of the modified structure can be measured; therefore, only the scaling factors $\alpha_{i,00}$ or $\alpha_{i,11}$ can be calculated.

If both $\{\phi_i\}$ and $\{\phi_{i,M}\}$ can be measured, then $\alpha_{i,01}$ is the most accurate, as shown in [17].

Another method can be obtained by using the approximation:

$$\frac{(\omega_i^2 - \omega_{i,M}^2)}{\omega_{i,M}^2} \approx \frac{2(\omega_i - \omega_{i,M})}{\omega_i} \tag{8}$$

in Equation (5), the equation:

$$\alpha_{i,p} = \sqrt{\frac{2(\omega_i - \omega_{i,M})}{\omega_i \{\psi_i\}^T [\Delta M]\{\psi_i\}}} \tag{9}$$

for the calculation of the scaling factor $\alpha_{i,p}$ is derived as proposed by Parloo *et al.* [12]. Equation (9) gives less accurate results than (5), (6) and (7), because of the approximation (8).

Lopez-Aenlle *et al.* [24] also mention other improved methods for the calculation of the scaling factors. One of them is the Bernal projection equation [25] that gives good estimates of the scaling factor $\alpha_{i,b}$ even in cases when the mode shapes change significantly. The Bernal projection equation is shown in (10):

$$\alpha_{i,b} = \sqrt{\frac{(\omega_i^2 - \omega_{i,M}^2)B_{ii}}{\omega_{i,M}^2 \{\psi_i\}^T [\Delta M]\{\psi_{i,M}\}}} \tag{10}$$

B_{ii} represents the i-th diagonal element of the matrix $[B]$. The matrix $[B]$ is calculated as shown in Equation (11), where $[\Psi]$ denotes the modal matrix of the unmodified mode shapes $\{\psi_i\}$ and $[\Psi_M]$ the modal matrix of the modified mode shapes $\{\psi_{i,M}\}$:

$$[B] = [\Psi]^{-1}[\Psi_M] \tag{11}$$

2.2. Operational mode-shape normalisation of small and light structures

The mass-change strategy with the scaling factors shown in Equations (5)-(7) gives relatively good results for most of the structures, as shown by Coppotelli [22]. But when small and light structures are analysed (Figure 1), the mass of the accelerometer can be relatively large in comparison to the other masses added to the structure for the normalisation [10]. Therefore, the added mass is not well distributed over the structure and not only do the resonant frequencies change, but also the mode shapes. The condition $\{\psi_i\} \approx \{\psi_{i,M}\}$ is not fulfilled, which leads to incorrect scaling factors α_i (Figure 1). The mass of the accelerometer for the mass-change strategy is also considered as the added mass to the structure in Figure 1 (left). Parloo *et al.* [12] performed the mass-change strategy with the accelerometers on the unmodified and the modified structure, because the mass of the accelerometer was negligible. The mass-change strategy presented in Figure 1 (left) is therefore even more favourable for small and light structures, because it reduces the influence of the added mass of the accelerometer on the measured modal parameters. However, when the mass of the accelerometer is larger than the other added masses for the mass-change strategy the scaling factors still need correction.

To correctly measure and normalise the mode shapes of the structure itself an improved method that can serve as an upgrade of the mass-change strategy is proposed in this study. The mass-change strategy is performed on the structure with the accelerometer. The added mass is well distributed over the modified structure; therefore, the mode shapes of the unmodified and modified structure do not differ significantly (the condition $\{\psi_i\} \approx \{\psi_{i,M}\}$

10

is fulfilled). Consequently, the scaling factors α_i are correct and the mode shapes of the structure with the accelerometer can be normalised. Then the variation of the mode shapes due to the added mass of the accelerometer needs to be determined and the normalised mode shapes $\{\phi_i^*\}$ of the structure itself (without the accelerometer) can be obtained. A proper method is needed to determine the mode-shape variation due to the accelerometer's added mass. The variation of the resonant frequencies due to the accelerometer's added mass can be taken into account by measuring the resonant frequencies of the structure itself (without the accelerometer) using only the LDV or by employing the same methods as for the mode-shape variation. Therefore, different methods for the variation of the modal parameters proposed by He [26], Aryana and Bahai [27] and Chen [28] were analysed in Section 2.3 in order to choose the right one for this study. The method proposed in this study is useful for the cases, when the OMA is performed by an accelerometer and an LDV. Then the accelerometer added mass should be cancelled by a mode-shape variation method. However, if there is a possibility of using two LDVs for the OMA, then the mode shapes of the structure without the accelerometer can be measured. In that case the Bernal projection equation (10) should be used to correctly normalise the mode shapes and the mode shape variation is already taken into account by that equation.

2.3. Variation of the modal parameters due to a structural modification

If the changes in the structural parameters from the initial to the modified structure are relatively small, then the sensitivity-analysis technique or other similar methods with a first-order approximation can be used to calculate the variation of the modal parameters, as shown by He [26]. But when

11

the structural modifications are larger, these approximations do not produce results that are good enough, as pointed out by Maia and Silva [2] and Aryana and Bahai [27]. Therefore, Chen [28] proposed an iterative procedure to provide exact predictions for the resonant frequencies and the corresponding mode shapes of the modified structure. Additionally, Chen [28] presented a high-order approximation approach, which gives better results compared to the sensitivity analysis, but still not as good as the aforementioned iterative procedure, which was also used in this study.

Chen's iterative procedure gives approximations of the i-th modified eigenvalue λ_i^* and eigenvector $\{\phi_i^*\}$, which are determined on the basis of the i-th unmodified eigenvalue λ_i and eigenvector $\{\phi_i\}$ of the structure. The procedure is presented in Equations (12) and (13).

$$\lambda_i^* = \lambda_i + \Delta\lambda_i \tag{12}$$

$$\{\phi_i^*\} = \{\phi_i\} + \sum_{k=1,k\neq i}^{N} C_{ik}\{\phi_k\} \tag{13}$$

The i-th eigenvalue $\lambda_i = \sqrt{\omega_i^2(1 + \mathrm{i}\eta_i)}$ contains the information on the resonant frequency ω_i and the damping loss factor η_i; the eigenvector $\{\phi_i\}$ represents the i-th normalised mode shape. The modification of the i-th eigenvalue is denoted by $\Delta\lambda_i$ and the modification of the i-th eigenvector can be expressed as a linear combination of all the independent original eigenvectors except for the corresponding one ($k \neq i$). C_{ik} is a participation factor of the k-th eigenvector when calculating the modification of the i-th eigenvector. The definitions of the modifications of the eigenvalues $\Delta\lambda_i$ and the participation factors C_{ik} are presented in Equations (14) and (15), de-

12

rived by Chen [28], where a_{ki}^K and a_{ki}^M are defined as shown in Equations (16) and (17).

$$\Delta\lambda_i = \frac{\left(a_{ii}^K - \lambda_i a_{ii}^M\right) + \sum_{k=1,k\neq i}^{N}\left(a_{ki}^K - \lambda_i a_{ki}^M\right)C_{ik}}{1 + a_{ii}^M + \sum_{k=1,k\neq i}^{N} a_{ki}^M C_{ik}} \tag{14}$$

$$C_{ik} = \frac{\left(a_{ki}^K - \lambda_i^* a_{ki}^M\right) + \sum_{l=1,l\neq i,k}^{N}\left(a_{kl}^K - \lambda_i^* a_{kl}^M\right)C_{il}}{\left(\lambda_i^* - \lambda_k\right) - \left(a_{kk}^K - \lambda_i^* a_{kk}^M\right)} \tag{15}$$

$$a_{ki}^K = \{\phi_k\}^T[\Delta K]\{\phi_i\} \tag{16}$$

$$a_{ki}^M = \{\phi_k\}^T[\Delta M]\{\phi_i\} \tag{17}$$

It is clear from Equations (14) and (15) that the calculations of $\Delta\lambda_i$ and C_{ik} do not require a knowledge of the mass and stiffness matrices of the original or modified structures. It is sufficient to know the modification of these two matrices ($[\Delta M]$ and $[\Delta K]$). The whole iterative procedure is done by repeatedly alternating between (14) and (15) until the convergence criterion presented in Equation (18) is satisfied (ε is the convergence tolerance). In the first approximation of $\Delta\lambda_i$ we use the value $C_{ik} = 0$ for all i and k.

$$\frac{\left|\Delta\lambda_i^{(n)} - \Delta\lambda_i^{(n-1)}\right|}{\left|\lambda_i + \Delta\lambda_i^{(n)}\right|} \prec \varepsilon \tag{18}$$

The described iterative procedure of Chen ensures an accurate estimation of the mode-shape variation due to the structural modification. For this reason it was used in this study to determine the mode-shape variation caused by the additional mass of the accelerometer.

13

3. Sample

To compare the experimental approaches EMA, OMA and the numerical model, a sample of simple geometry with the proper geometrical and modal characteristics was needed. A steel sample of circular cross-section with 6-mm diameter, 108-mm length and 21-gram mass was used, as shown in Figure 2. Its geometry was chosen in such a way as to ensure one axial-mode, one torsional-mode, and many bending-mode shapes in the frequency range of the measurement (0-20 kHz). The sample has a small, narrower section where the diameter is reduced to 1.4 mm (to lower the first axial resonant frequency under 20 kHz) and two grooves (introducing axial asymmetry). In this study the focus will only be on the first five bending-mode shapes in the direction of the Y axis. Other mode shapes and resonant frequencies can be measured in the same manner. Fifteen points on the structure, which are shown in Figure 2, were used for the measurements; therefore, the results of the model will also be calculated for these points. The sample that was used for this study is a homogenous structure without any joints. It has well-known material characteristics and geometry; therefore, a relatively accurate FEM was formed based on this.

4. Numerical experiment

The variation of the mode shapes due to the added mass was simulated using the numerical model, and the correct functioning of Chen's method, proposed in Section 2.3, was verified.

4.1. Modal analysis

An FEM model was built based on the geometrical and material parameters of the sample. A numerical modal analysis was performed on the model to determine the resonant frequencies and the normalised mode shapes. Viscous damping with a constant damping ratio of 3 % was introduced to the model, taking into account the results of the measurement. The modal parameters were determined for the structure without the added mass (load case A) and for the structure with the added mass of the accelerometer at point 15 (load case B). The added mass of the accelerometer was simulated with a single-node finite element that represents a concentrated mass. The total added mass of the accelerometer, which was used for the OMA, was estimated to be 1 gram (0.7 gram accelerometer and 0.3 gram connecting cable). Therefore, this value was also used for the load case B of the numerical model. Since the damping is based on the results of the measurement, it is reasonable to compare the resonant frequencies and mode shapes only. The resonant frequencies can be seen in Table 1 and the corresponding mode shapes in Figure 3. The mode shapes are denoted with indexes num-A (representing the numerical model load case A), num-B (representing the numerical model load case B), and num-B* (representing num-B with cancelled load of the accelerometer). The mode shapes num-B* were determined by using the Chen's method for the cancellation of the accelerometer's added mass on the num-B mode shapes. The correlation of the mode shapes was calculated using the Modal Assurance Criterion (MAC) [29, 30]. Figure 4 shows the correlation between the mode shapes of the structure with the added mass (load case B) and without the added mass (load case A). The diagonal MAC

15

values are presented in Table 2.

Table 1: Comparison of resonant frequencies calculated with the numerical model for load cases A (without the added mass) and B (with the added mass of the accelerometer at point 15).

Resonant frequency No.	Load case A	Load case B
1.	383 Hz	357 Hz
2.	3552 Hz	3446 Hz
3.	6905 Hz	6826 Hz
4.	16986 Hz	15463 Hz
5.	18273 Hz	17594 Hz

Table 2: Diagonal MAC values of the numerical mode shapes.

	Diagonal MAC value	
Mode No.	num-A, num-B	num-A, num-B*
1.	0.98	0.98
2.	0.99	0.99
3.	0.99	1.00
4.	0.72	0.93
5.	0.50	0.93

It is clear from Figure 4 that the fifth mode shape (left MAC matrix) has a diagonal MAC value significantly lower than 1, which proves that the mode shapes are not well correlated, because a change of the mode shapes

16

occurs due to the additional mass of the accelerometer. If this structural modification is not taken into account, then the measured operational mode shapes agree with the load case B. But the goal is to measure the mode shapes without the added mass (load case A). Chen's method, which is described in Section 2.3, was used to calculate the variation of the modal parameters due to the added mass of the accelerometer. The calculated mode shapes were transformed from B (with the added mass of the accelerometer) to B* (the added mass of the accelerometer is cancelled) as demonstrated in Figure 3. Figure 4 indicates that B* is well correlated to A, because all the diagonal elements of the right MAC matrix are very close to 1 and the others are close to 0. Chen's method is therefore suitable for this study and it can be used on the measurement results, as it correctly calculates the variation of the mode shapes due to the structural modification.

5. Experimental investigation

The aim of the experimental investigation was to analyse the advantages and disadvantages of the proposed method for the normalisation of the operational mode shapes in comparison to the mass-change strategy (as demonstrated by Parloo *et al.* [12] and Lopez-Aenlle *et al.* [16]) and also to classic EMA [2] with a known excitation, because EMA is the most frequently used method.

5.1. EMA

Measurements of the FRFs were required for the EMA. During these measurements the excitation force and the response (velocity) of the structure were monitored simultaneously. The sample was suspended by two strings

17

to simulate the free-free support, as shown in Figure 5. The white noise excitation was carried out in the horizontal direction with the use of the LDS V-101 electromagnetic shaker that was also suspended by two strings. The measurement of the response was performed using a LDV Polytec PDV-100 at fifteen points (1-15) in the Y direction, as shown in Section 3 (Figure 2). The measurement points were the same for the OMA. The structure was excited at point 9 for the EMA. The Ewins-Gleeson method [1, 2] was used to identify the modal parameters from the measurements.

A custom-made sensor was developed to measure the excitation force and transfer it from the shaker to the sample. This sensor is based on a piezo strain gauge (PCB 740B02). Its structure and functioning are described in an article by Rovšček *et al.* [11], where a detailed description of the EMA procedure can also be found. The effect of the added mass of the force sensor on the structure was small (0.4 gram) and neglected in the calculation of the modal parameters.

5.2. OMA

The sample was suspended by two strings when performing the OMA, as shown in Figure 6. The ambient excitation was carried out using a small steel ball (4 mm diameter) that was glued to a string and swung into the structure to achieve impact excitation. The steel ball hit the structure in point 9 (Figure 2), where all the measured modes were excited well. Exciting the structure with an impact in the same point is in general not a good practice (as some of the vibration modes would possibly not be excited). However, when small and light structures are measured, the position change of the excitation point can result in relatively high variations of the force

18

load (amplitude and direction). The variation of the excitation force results in the decrease of the quality of the analysis. In this research better results have been achieved by carefully selecting the excitation point and then excite the system always at that selected point. The reference response was measured by a B&K 4517-002 accelerometer, which was positioned at point 15. The response at the i-th point on the structure ($i = 1, 2, 3, \ldots, 15$) was measured using a LDV Polytec PDV-100. From the reference response and the response at the i-th point on the structure the operating deflection shape FRFs (ODS FRFs) were obtained. The ODS FRFs were scaled by considering the variations in the load between the measurement sets as proposed by Schwarz and Richardson [31], which contributed to a better accuracy. The resonant frequencies ω_i and unnormalised mode shapes $\{\psi_i\}$ were extracted from the scaled ODS FRFs. The ODS FRFs can be curve fit using an FRF curve-fitting model, as shown by Schwarz and Richardson [31], because the excitation force spectrum can be assumed to be relatively constant in the frequency range of the modes of interest. Therefore, the Ewins-Gleeson method was used for the OMA, just like for the EMA. For the normalisation of the mode shapes with the mass-change strategy, eight magnets, each with a mass of 0.21 gram, were added at points 1, 3, 5, 7, 9, 11, 13 and 15 on the structure and the resonant frequencies $\omega_{i,M}$ of the changed structure were measured. Then the scaling factors $\alpha_{i,00}$ were calculated, as shown in Equation (5), to normalise the operational mode shapes of the structure with the accelerometer at point 15 (load case B). The mode shapes of the structure itself (without the accelerometer - load case B*) were obtained by using the method described in Section 2.3.

The aim of this study was to take into consideration the mode-shape variation, which occurs on small and light structures while performing the OMA (because of the added mass of the accelerometer). The accelerometer was therefore deliberately placed at the point 15 to achieve sufficient modification of the mode shapes to clearly present the advantages of the proposed method. Point 15 is otherwise not the best position for this sensor to obtain good results with the OMA.

5.3. Comparison of the results

5.3.1. Resonant frequencies

The comparison of the resonant frequencies calculated with the numerical model and measured with the EMA and OMA is presented in Table 3. The resonant frequencies for OMA-A (where A denotes the load case) were measured only with the LDV (without the added mass of the accelerometer). All the other OMA measurements were performed with the accelerometer and the LDV, as described in Section 5.2.

Table 3: Comparison of resonant frequencies calculated with the numerical model and measured with the EMA and OMA.

Res. freq. No.	num-A	num-B	EMA	OMA-A	OMA-B
1.	383 Hz	357 Hz	379 Hz	377 Hz	358 Hz
2.	3552 Hz	3446 Hz	3538 Hz	3550 Hz	3446 Hz
3.	6905 Hz	6826 Hz	6795 Hz	6900 Hz	6818 Hz
4.	16986 Hz	15463 Hz	17058 Hz	17100 Hz	15366 Hz
5.	18273 Hz	17594 Hz	18612 Hz	18622 Hz	17506 Hz

It is clear from Table 3 that the resonant frequencies of the structure without the accelerometer (num-A, EMA and OMA-A) differ by less than 2 %. The resonant frequencies of the structure with the accelerometer at point 15 (num-B, OMA-B) are even closer together (less than 0.7 % difference). Therefore, the measured values of the resonant frequencies are accurate in both cases, EMA or OMA.

5.3.2. Mode shapes

The results of the EMA will be discussed first. In Figures 7 and 8 the mass-normalised mode shapes that were measured with the EMA are compared to those that were calculated with the numerical model. The diagonal MAC values are presented in Table 4. The results show that all the mode shapes in the frequency range of the sensor (500 Hz - 20 kHz) are well correlated with those of the numerical model (the diagonal MAC values are over 0.9). The first mode shape is below 500 Hz; therefore, the correlation is not as good as for the modes 2-5 (the diagonal MAC value is just 0.67). The first mode is the most dominant; therefore, it should be measured with better accuracy. The first five bending-mode shapes in the direction of the Y axis can be measured with the described EMA procedure, but the goal of the proposed OMA procedure is to improve these measurements, especially the measurement of the 1st mode shape and the mass normalisation of 4th and 5th mode shapes.

The results of the OMA were also compared with those of the numerical model. The mode shapes were measured for load case B (with the added mass of the accelerometer), since this measurement for A is not possible when using an accelerometer. The comparison of the measured (OMA) and

Table 4: Diagonal MAC values of the numerical, OMA and EMA mode shapes.

Mode No.	Diagonal MAC value		
	num-A, EMA	num-A, OMA-B	num-A, OMA-B*
1.	0.67	0.99	0.99
2.	0.99	0.98	0.96
3.	0.96	0.98	0.97
4.	0.94	0.69	0.82
5.	0.91	0.52	0.71

the calculated mode shapes is presented in Figures 9 and 10. The diagonal MAC values are presented in Table 4.

In Figure 9 it is clear that the scale of the numerical and OMA mode shapes are similar; however, the scale of the EMA mode shapes is rather different for the 4th and 5th mode shape, as shown in Figure 7. The similarity of the numerical and OMA mode shapes confirms that the scale factors $\alpha_{i,00}$ were calculated correctly. If the numerical load case A (without the added mass) is compared to the OMA measurement results (load case B) the correlation is not so good, as shown in Figure 10 (left). If the variation of the modal parameters because of the structural modification is taken into account, then the mode shapes OMA-B transform into OMA-B*. Figure 10 (right) and Table 4 show that OMA-B* is better correlated with num-A than OMA-B. All the diagonal MAC values are above 0.71 (the first three even above 0.95) and the diagonal MAC value for the 4th and 5th modes change from 0.69 and 0.52 to 0.82 and 0.71. Also, the non-diagonal values of the

MAC matrix are lowered; therefore, there is better orthogonality of the mode shapes. This proves that the procedure proposed in this study can be used to measure the mass-normalised mode shapes of small and light structures, even if the variation of the mode shapes occurs during the measurement. This variation is usually caused by the added mass of the sensors.

Table 5: Diagonal MAC values of the numerical mode shapes.

	Diagonal MAC value	
Mode No.	EMA, OMA-B	EMA, OMA-B*
1.	0.70	0.70
2.	0.99	0.97
3.	0.95	0.98
4.	0.53	0.66
5.	0.28	0.48

When the results of the OMA are compared with the results of the EMA, as shown in Figure 11 and Table 5, it is clear that a better correlation of the mode shapes is achieved if the variation of the modal parameters is taken into account. This confirms that the consideration of the accelerometer's added mass significantly improves the results.

6. Conclusion

This study presents an improved procedure for an operational mode-shape normalisation. This procedure takes into account the mode-shape variation

that occurs because of the additional mass of the accelerometer. It is advisable to use the proposed method when the mass that is added to the structure by the accelerometer is not negligible. The measurement of the excitation force is not needed, which makes the experimental investigation even more straightforward and easy to perform.

The presented method was first tested on the numerical model. The results show that the correlation of the mode shapes is much better if the variation of the modal parameters due to a structural modification is taken into account. The sample that was used to build the numerical model was later used for the EMA and OMA measurements. The measurement results were compared with the numerical model and between the EMA and OMA. The comparison proves that the method proposed in this study gives better results than the ordinary mass-change strategy, because the sensor's additional mass is cancelled and the mode shapes are scaled correctly. The proposed method can be used on similar small and light structures and also on larger structures. This method is important when a mode-shape variation due to the additional mass of the sensor occurs.

Acknowledgements

References

[1] D. J. Ewins, Modal Testing: Theory and Practice, Research Studies Press, John Wiley and Sons, Lechtworth, New York etc., 1984.

[2] N. M. M. Maia, J. M. M. Silva, Theoretical and Experimental Modal Analysis, Research Studies Press, John Wiley and Sons, Taunton, New York etc., 1997.

[3] J. He, Z.-F. Fu, Modal Analysis, Butterworth-Heinemann, Oxford, Boston etc., 2001.

[4] B. J. Schwarz, M. H. Richardson, Introduction to operating deflection shapes, Computational Systems Inc. Reliability Week, Orlando, FL (USA) (1999).

[5] R. Brincker, N. Møller, Operational modal analysis - a new technique to explore, Sound and Vibration 40 (2006) 5–6.

[6] R. Brincker, P. Andersen, A Way of Getting Scaled Mode Shapes in Output Only Modal Testing, Proceedings of IMAC-21: A Conference on Structural Dynamics (2003) 141–145.

[7] C. J. Wilson, D. B. Bogy, An experimental modal analysis technique for miniature structures, Journal of Vibration and Acoustics - Transactions of the ASME 118 (1996) 1–9.

[8] T. M. Huber, M. Fatemi, R. Kinnick, J. Greenleaf, Noncontact modal analysis of a pipe organ reed using airborne ultrasound stimulated vi-

brometry, Journal of Acoustical Society of America 119 (2006) 2476–2482.

[9] O. B. Ozdoganlar, B. D. Hansche, T. Carne, Experimental modal analysis for microelectromechanical systems, Experimental Mechanics 45 (2005) 498–506.

[10] J. M. M. Silva, N. M. M. Maia, A. M. R. Ribeiro, Cancellation of mass-loading effects of transducers and evaluation of unmeasured frequency response functions, Journal of Sound and Vibration 236 (2000) 761–779.

[11] D. Rovšček, J. Slavič, M. Boltežar, The use of strain sensors in an experimental modal analysis of small and light structures with free-free boundary conditions [published online ahead of print april 27, 2012], Journal of Vibration and Control, DOI: 10.1177/1077546312445058 (2012).

[12] E. Parloo, P. Verboven, P. Guillaume, M. Van Overmeire, Sensitivity-based operational mode shape normalisation, Mechanical Systems and Signal Processing 16 (2002) 757–767.

[13] E. Parloo, B. Cauberghe, F. Benedettini, R. Alaggio, P. Guillaume, Sensitivity-based operational mode shape normalisation: Application to a bridge, Mechanical Systems and Signal Processing 19 (2005) 43–55.

[14] E. Parloo, P. Guillaume, J. Anthonis, W. Heylen, J. Swevers, Modelling of sprayer boom dynamics by means of maximum likelihood identification techniques, Part 1: A comparison of input-output and output-only modal testing, Byosistems Engineering 85 (2003) 163–171.

[15] E. Parloo, P. Guillaume, J. Anthonis, W. Heylen, J. Swevers, Modelling of sprayer boom dynamics by means of maximum likelihood identification techniques, part 2: Sensitivity-based mode shape normalisation, Byosistems Engineering 85 (2003) 291–298.

[16] M. Lopez-Aenlle, P. Fernandez, R. Brincker, A. Fernandez-Canteli, Scaling-factor estimation using an optimized mass-change strategy (Correction of: 24(5), p. 1260-1273, 2010), Mechanical Systems and Signal Processing 24 (2010) 3061–3074.

[17] M. Lopez-Aenlle, R. Brincker, A. Fernandez-Canteli, L. M. V. Garcia, Scaling-factor estimation by the optimized mass-change method, Proceedings of IOMAC-1 (2005) 53–64.

[18] M. Lopez-Aenlle, R. Brincker, A. Fernandez-Canteli, Some methods to determine scaled mode shapes in natural input modal analysis, Proceedings of IMAC-23: A Conference on Structural Dynamics (2005) 141–145.

[19] M. Lopez-Aenlle, P. Fernandez, R. Brincker, A. Fernandez-Canteli, Scaling-factor estimation using an optimized mass-change strategy, Part 1: Theory, Proceedings of IOMAC-2 (2007) 421–428.

[20] P. Fernandez, M. Lopez-Aenlle, L. M. V. Garcia, R. Brincker, Scaling-factor estimation using an optimized mass-change strategy, Part 2: Experimental Results, Proceedings of IOMAC-2 (2007) 429–436.

[21] P. Fernandez, P. Reynolds, M. Lopez-Aenlle, Scaling Mode Shapes in Output-Only Systems by a Consecutive Mass Change Method, Experimental Mechanics 51 (2011) 995–1005.

[22] G. Coppotelli, On the estimate of the FRFs from operational data, Mechanical Systems and Signal Processing 23 (2009) 288–299.

[23] M. M. Khatibi, M. R. Ashory, A. Malekjafarian, R. Brincker, Mass-stiffness change method for scaling of operational mode shapes, Mechanical Systems and Signal Processing 26 (2012) 34–59.

[24] M. Lopez-Aenlle, R. Brincker, F. Pelayo, A. Fernandez-Canteli, On exact and approximated formulations for scaling-mode shapes in operational modal analysis by mass and stiffness change, Journal of Sound and Vibration 331 (2012) 622–637.

[25] D. Bernal, Modal scaling from known mass perturbations, Journal of Engineering Mechanics 130 (2004) 1083–1088.

[26] J. He, Structural modification, Philosophical Transactions of the Royal Society A: Mathematical, physical and engineering sciences 359 (2001) 187–204.

[27] F. Aryana, H. Bahai, Sensitivity analysis and modification of structural dynamic characteristics using second order approximation, Engineering structures 25 (2003) 1279–1287.

[28] H. P. Chen, Efficient methods for determining modal parameters of dynamic structures with large modifications, Journal of Sound and Vibration 298 (2006) 462–470.

[29] R. J. Allemang, The modal assurance criterion - Twenty years of use and abuse, Sound and Vibration 37 (2003) 14–23.

[30] D. Fotsch, D. J. Ewins, Application of MAC in the Frequency Domain, Proceedings of IMAC-18: A Conference on Structural Dynamics (2000) 1225–1231.

[31] B. J. Schwarz, M. H. Richardson, Measurements required for displaying operating deflection shapes, Proceedings of IMAC-22: A Conference on Structural Dynamics (2004) 701 – 706.

List of Figures

Figure 1: Comparison of the mass-change strategy and the method used in this study.
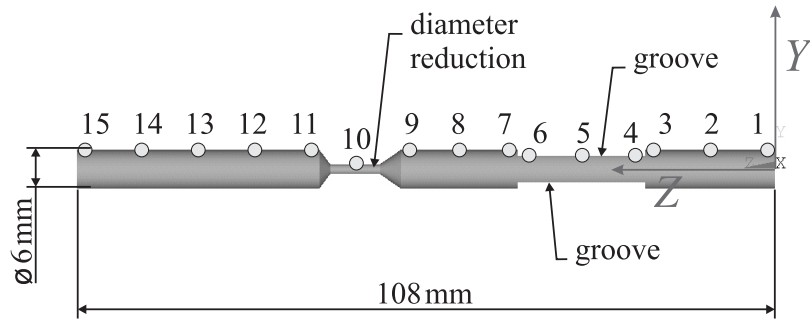
Figure 2: Sample under investigation.
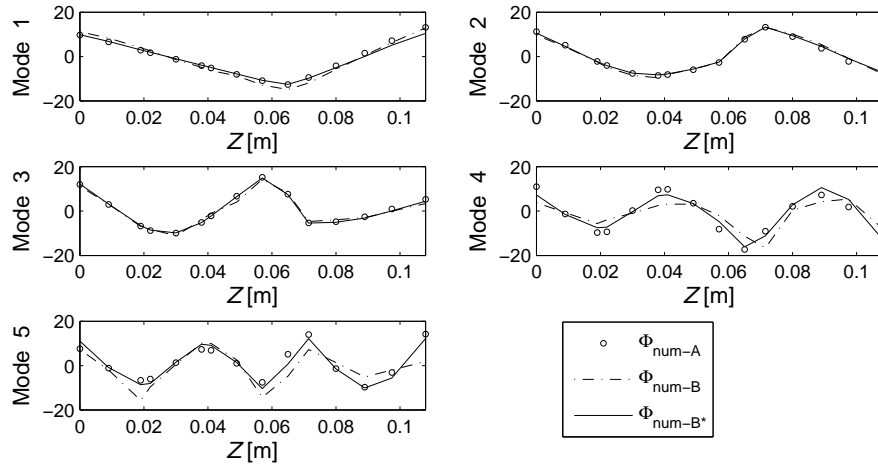
Figure 3: Transformation of the numerical mode shapes num-B into num-B* and comparison with num-A.
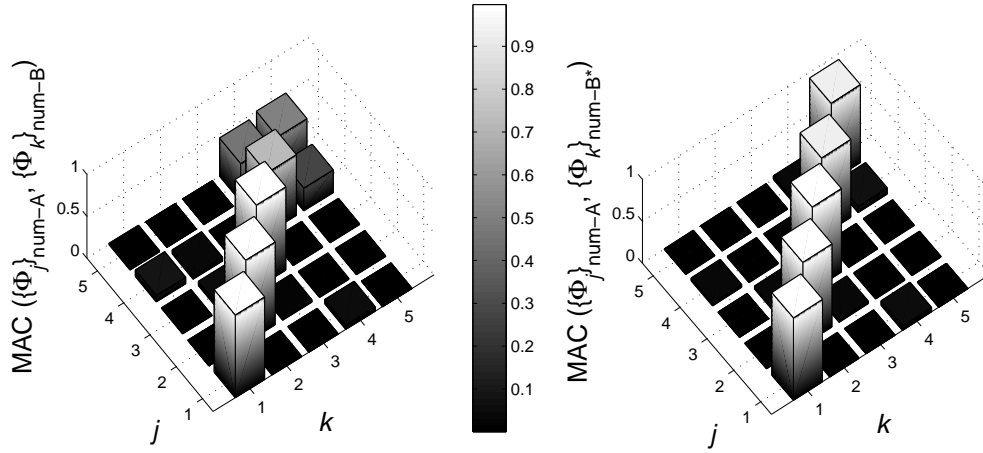
Figure 4: MAC correlation of numerical mode shapes for load case A and B and transformed mode shapes B*.
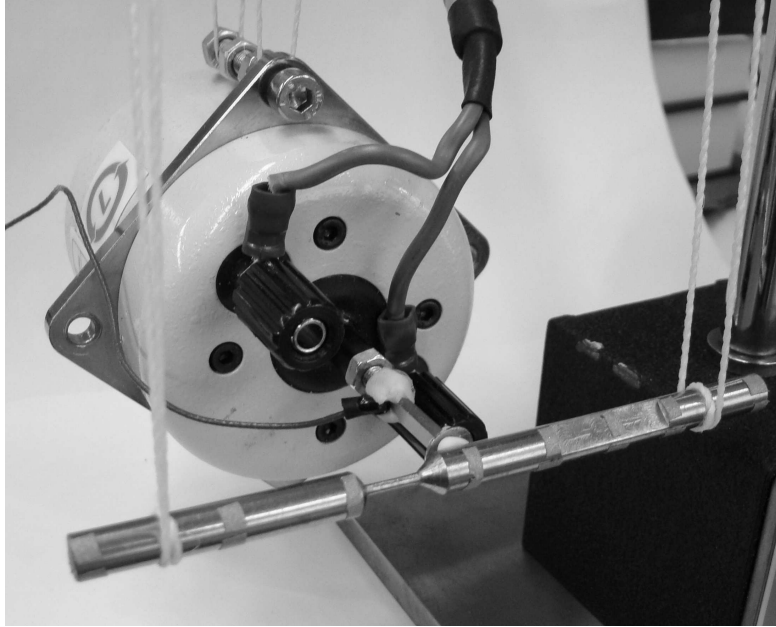
Figure 5: Experimental setup for the EMA.
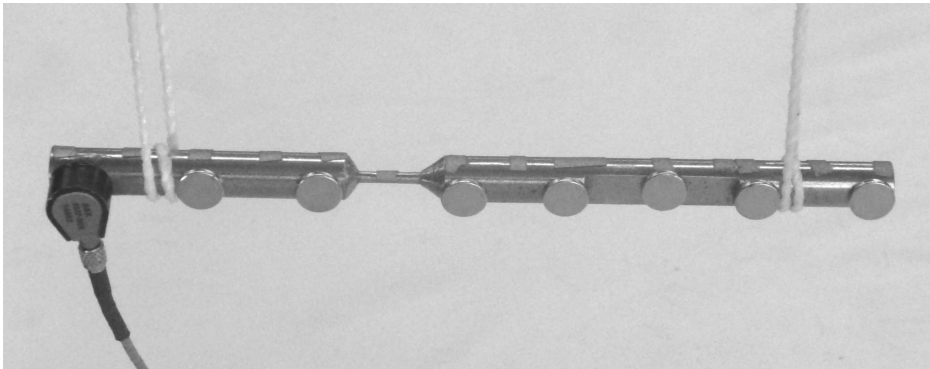
Figure 6: Experimental setup for OMA (with the magnets for the mass-change strategy).
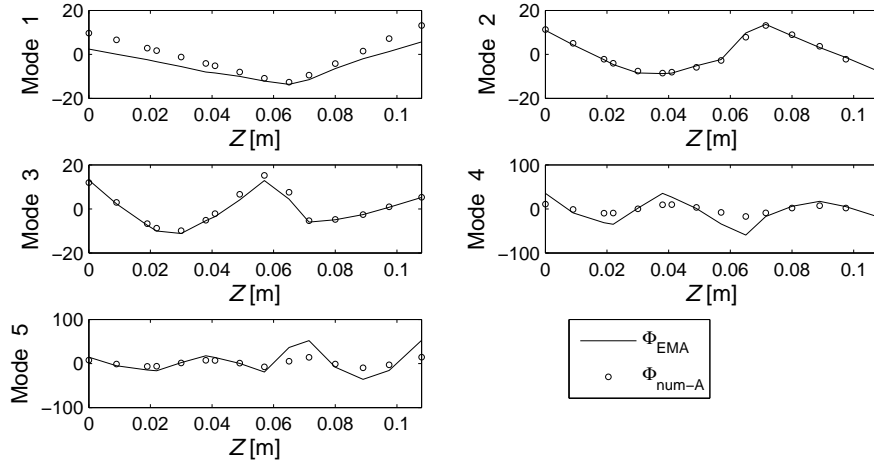
Figure 7: Mode shapes obtained with the EMA and a comparison with the numerical mode shapes of the structure itself (num-A).
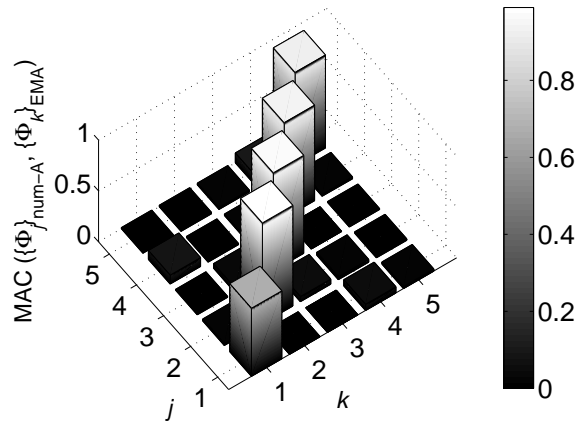
Figure 8: MAC correlation of num-A and EMA.
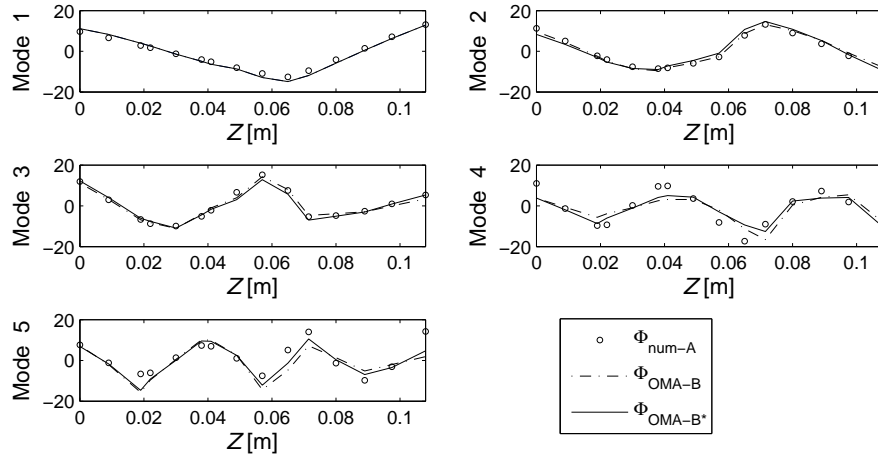
Figure 9: Numerical (num-A) and operational (OMA-B, OMA-B*) mode shapes.
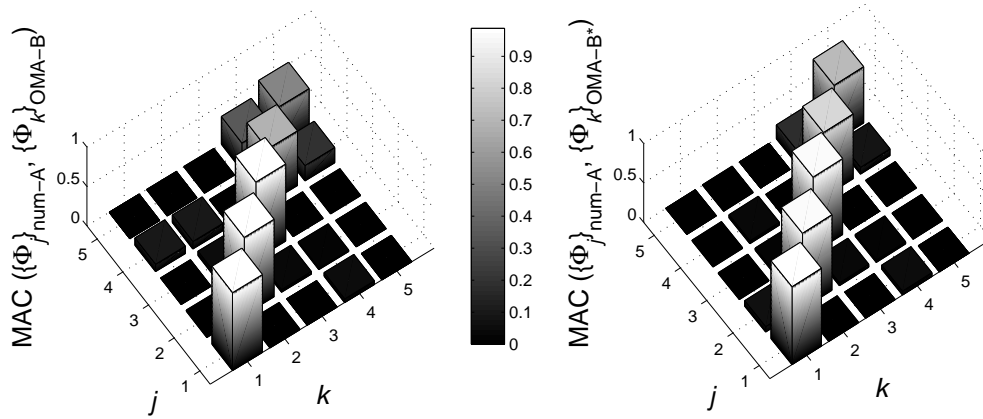
Figure 10: MAC correlation between numerical (num-A) and operational (OMA-B and OMA-B*) mode shapes.
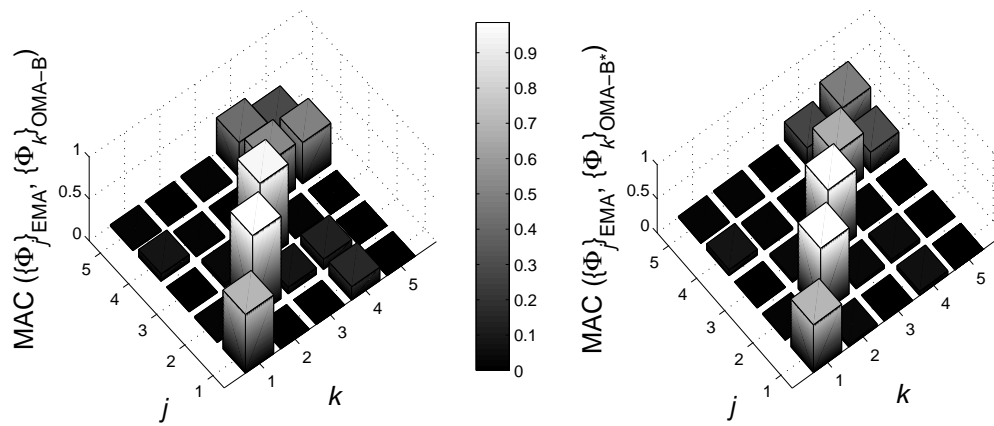
Figure 11: MAC correlation between experimental (EMA) and operational (OMA-B and OMA-B*) mode shapes.